Dual-Wavelength Speckle-Based SI-POF Sensor for Cost-Effective Detection of Microvibrations

Plinio Jesús Pinzón, David Sánchez Montero, Alberto Tapetado, and Carmen Vázquez, *Senior Member, IEEE*

***Abstract*—In this work, a novel method for cost-effective remote sensing of microvibrations is presented. The proposed technique detects periodical changes in the spatial distribution of energy on the speckle pattern at the endface of a SI-POF. By employing a dual-wavelength approach it is possible to increase the system sensitivity without changing its maximum mean squared error, which increases the system accuracy as well as its resolution. The system operates in reflective configuration providing a centralized interrogation scheme. The speckle pattern of both wavelengths is demultiplexed at the fiber end before being directly recorded by an off-the-shelf and a cost-effective webcam. The changes in the intensity distribution are processed at the remote interrogation unit. The proposed system is able to detect instantaneous and periodic microvibrations (with amplitudes ranging from 1 to 6 μm) localized farther than 9 m from the remote interrogation unit.**

***Index Terms*—Cost-effective, dual-wavelength, plastic optical fiber, speckle pattern, vibration measurements.**

I. Introduction

When a highly coherent light propagates through a multimode optical fiber via a number of modes interference between these modes yields a speckle pattern, so–called modal noise, at the fiber end–face. This speckle pattern is extremely sensitive to the phase difference among the propagated modes, which can arise from time–varying fiber disturbances resulting from external forces or thermal drifts, among others. Since this negative effect was early reported by Takahara [1] and Epworth [2] extensive efforts have been dedicated to overcome its dramatic impact in optical communication systems. However since the speckle pattern measured at the fiber end is extremely sensitive to any disturbances along the fiber, the sensing community has envisioned this physical effect to be potentially suitable to measure a wide range of measurands (pressure, temperature, vibration, etc.).

Fiber-optic sensors are evolving rapidly. This is mainly because of the inert nature of optical fibers that allows electromagnetic immunity, biocompatibility and safe applications in harsh and inflammable atmospheres. In recent years it has been shown that polymer optical fibers (POFs) have multiple applications in sensing systems at a very low or competitive cost compared to the well established conventional technologies. POF based sensors nowadays play an important role in applications such as structural health monitoring, biomedicine [3], environmental and biochemical areas.

Among the different POF types, the standard step index POF (SI–POF) with a 980 μm core diameter of polymethyl–methacrylate (PMMA) and numerical aperture (*NA*) of $\sim$0.47 offers several advantages thanks to its potential low cost which allows easiness of handling, installation, splicing and connecting. SI–POF is mainly used in the visible spectrum range where it shows an acceptable attenuation and different passive devices have been designed [4].

Most recent speckle–based POF sensors have been developed to pressure monitoring in petrol pipes [5] or to measure the temperature at the surface of a metal plate through a correlation coefficient [6]. Speckle analysis for monitoring vital signs of patients [7] and in combination with fiber Bragg gratings (FBG) [8] to measure strain have also been reported. Due to the high sensitivity of speckle pattern changes, this can be a drawback in final applications due to the random nature of the interference of the fiber modes produced by ambient perturbations as well as the modal noise of the light source. Up to now, only single wavelength speckle patterns are reported. Reflective configurations have been proposed to increase sensitivity in different sensing configurations [9], [10]. They can be used to develop more compact schemes for the same optical path and a centralized remote interrogation for multiple micro-vibration detection.

In this work a novel dual–wavelength speckle–based sensing technique is proposed for remote detection of micro–vibrations. Additionally, the scheme operates in reflective configuration thus performing a centralized interrogation unit scheme. The proposed technique detects periodical changes in the spatial distribution of energy on the speckle pattern in the output of a SI–POF. It is shown that the dual–wavelength approach allows increasing the system accuracy as well as enhancing its resolution.

II. System Description

Fig. 1 shows the general description of the proposed SI–POF based micro–vibration sensor. Two laser pointers (LDs), with $\lambda_1 = 532$ nm (Green) and $\lambda_2 = 650$ nm (Red) respectively, are multiplexed using a 50:50 coupler. Next the light beam composed by λ_1 and λ_2 is directed to a 3–dB loss beam splitter cube BS, so that 50% of the light's intensity is injected into the sensing fiber lead.

Manuscript received June 3, 2016; revised September 16, 2016; accepted September 16, 2016. Date of publication September 20, 2016; date of current version November 9, 2016. This work was supported in part by the Spanish Ministry of Economy and in part by the European Union Development Fund under grant TEC2015-63826-C3-2-R (MINECO/FEDER), and in part by the Comunidad de Madrid under grant S2013/MIT-2790.

The authors are with the Electronics Technology Department, Universidad Carlos III de Madrid, Madrid 28911, Spain (e-mail: ppinzon@ing.uc3m.es; dsmontero@ing.uc3m.es; atapetad@ing.uc3m.es; cvazquez@ing.uc3m.es).

Color versions of one or more of the figures in this paper are available online at http://ieeexplore.ieee.org.

Digital Object Identifier 10.1109/JSTQE.2016.2611596

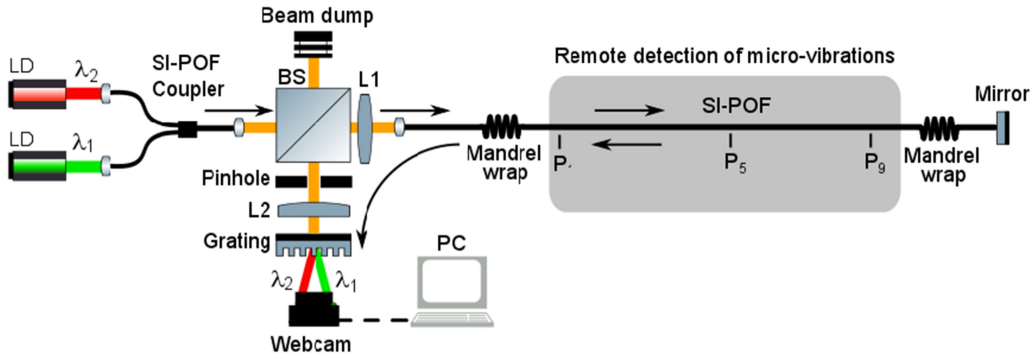

Fig. 1. Schematic of the proposed dual-wavelength speckle-based SI-POF sensor. Lenses L_1 and L_2 have focal lengths of 20 and 35 mm, respectively.

A standard PMMA SI–POF fiber with 980/1000 μm of core and cladding diameter, respectively, also including a jacket with 2.2 mm of diameter is used as sensing fiber lead. The fiber deployed has a total length of 11 m and includes two mandrel wraps, composed by six loops of 2.5-cm-diameter each, used to improve the modal distribution along the fiber and to eliminate possible unguided modes produced by the external disturbances along the fiber.

Finally, the mirror at the farthest end–face of the SI–POF reflects the light back to the fiber lead reaching the BS cube located at the interrogation unit which deflects 50% of the reflected intensity to the webcam.

The light beam reaching the webcam contains the speckle patterns of both λ_1 and λ_2. Both patterns are then demultiplexed and focalized on different spatial locations of the same webcam by using a transmission diffraction grating with groove density of 1200 lines/mm, as reported in [4]. The distance between both patterns is enough to be independently analyzed. Therefore, the proposed system allows analyzing two independent speckle patterns recorded at the same instant. This is a very useful approach to minimize the great impact of the random interference of fiber modes, i.e. modal noise.

III. Principle of Operation

The speckle patterns are a representation of the modal distribution at the end–face of the optical fiber. Although the total intensity of the patterns is approximately constant, their modal distribution is modified by external perturbations along the fiber lead, such as the temperature, pressure or displacement changes. The periodicity of such perturbations can be detected by analyzing the distribution of the speckle pattern over time at a single wavelength [11]. Moreover, if the disturbance suffered by the fiber is large enough to change the variance of the speckle pattern profile it is possible not only to detect but also locate the relative position of the perturbation source by analyzing the speckle pattern variance of two wavelengths [12].

The proposed method for remote detection of micro–vibrations using standard SI–POF fibers is based on computing the correlation factor between the time-varying speckle patterns recorded by the webcam with regards to a reference pattern, which is obtained by averaging N consecutive patterns. The correlation coefficients are calculated using the entire speckle patterns generated by each wavelength, defined as $Corr(G)$ and $Corr(R)$ for λ_1 and λ_2, respectively. This approach allows detecting small variations in the speckle pattern produced by micro–vibrations or micro–perturbations (temperature, pressure and displacement changes) along the sensing fiber.

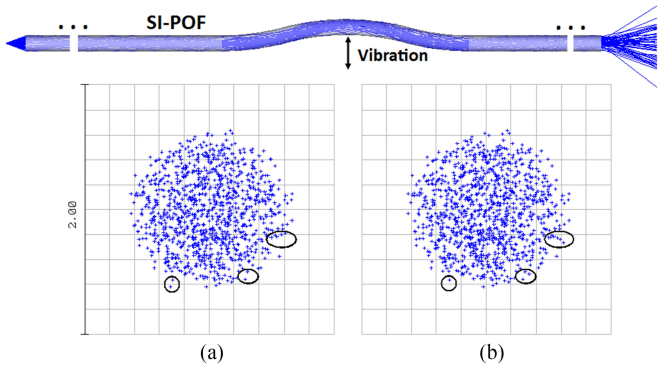

Fig. 2. Simulations of the speckle pattern variation in a SI–POF lead of 2 m, $\lambda = 520$ nm. The vibration's amplitude in b) is 1 μm greater than in a).

Fig. 2 shows an example of the modal distribution change that can arise in the speckle pattern of λ_1. The simulation was done using a ray tracing software considering the material and the geometric characteristics of a standard 2m-long SI–POF fiber. Circles within Fig. 2a and Fig. 2b show some examples of the changes in the modal distribution at the end–face of the optical fiber due to the influence of a 1 μm displacement. This simulation illustrates how the correlation factor of both patterns can be used to quantify the influence of micro–perturbations along the fiber lead.

By analyzing the entire pattern image at reception a highly sensitive sensing technique can be achieved, which is ideal for a cost–effective detection of remote micro–vibrations. However the high sensitivity could be an important drawback in final applications due to influence of ambient perturbations and light source modal noise. By analyzing the speckle pattern of two independent wavelengths that are recorded at the same time a reduction of the influence of the random noise in the system is achieved as demonstrated below.

IV. Experimental Setup and Measurements

The proposed SI–POF vibration sensor, see Fig. 1, has been tested using the experimental set-up shown in Fig. 3. A piezoelectric stack (with a maximum configurable displacement of

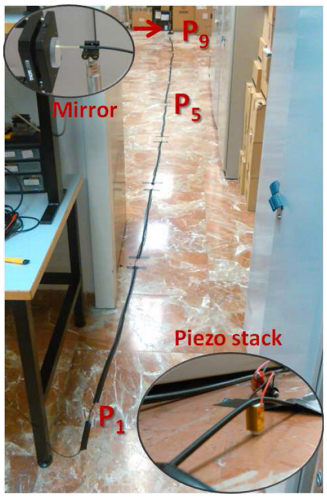

Fig. 3. Experimental set-up of the remote system for micro-vibrations detection. The sensing fiber is a standard SI-POF fiber of 11m-long with a 2.2 mm jacket directly attached to the floor. A piezoelectric stack is used to emulate periodic perturbations with amplitudes ranging from 1 to 6 um at points P_1, P_5 and P_9, respectively.

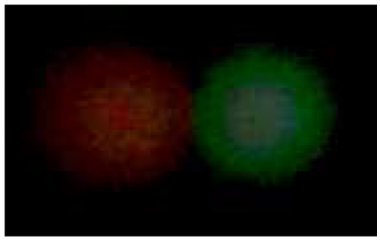

Fig. 4. Example of the speckle patterns of λ_1 (right, 520 nm) and λ_2 (left, 650 nm) recorded by the webcam. Both patterns are demultiplexed and then focused on the CCD camera sensor.

11.2 μm $\pm$ 15% and driving voltage range from 0 to 75 V) is used to generate periodic vibrations at 3 different points of the sensing fiber (named P_1, P_5 and P_9, respectively), separated in steps of 4 m each. The piezoelectric stack is driven by a sinusoidal signal of 2 Hz with a peak–to–peak amplitude $V_{\rm pp}$ and mean value $V_{\rm pp}/2$. The speckle patterns are recorded by an off–the–shelf and low cost USB webcam at 16.25 frames per second (fps) using a 320 $\times$ 240 pixels resolution and RGB color space. Fig. 4 shows an example of the speckle patterns of λ_1 and λ_2 recorded by the webcam at the centralized remote interrogation unit.

It is important to note that the sensing fiber lead was directly attached to the laboratory floor, except at the points where the piezoelectric stack was placed (see inner figure within Fig. 3), so it can be affected by other vibration sources (ambient noise). This was done in order to test the system performance in a realistic environment.

A. Data Processing

Once the images are recorded, the green (λ_1) and red (λ_2) reference patterns are obtained by averaging 20 consecutive speckle patterns. The averaging value has been experimentally chosen with the aim to improve the signal to noise ratio of the correlation coefficients without generating an excessive delay (<1.5 s). Then, the correlation coefficient between each color speckle pattern and its respective reference is calculated, by using the signals at each pixel in the illuminated area, thus obtaining *Corr*(*G*) and *Corr*(*R*) signals.

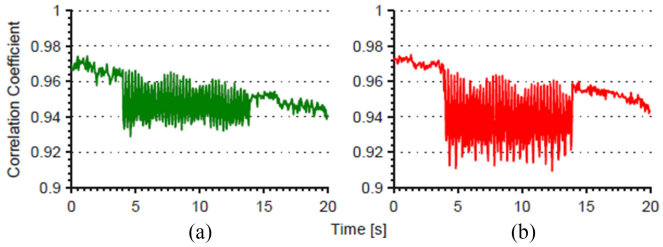

Fig. 5. Temporal behavior of the correlation coefficients: a) *Corr*(*G*) and b) *Corr*(*R*). The vibration source (with $\pm$5.6 μm amplitude, 2 Hz frequency and 20 s of duration) is located at point P_5.

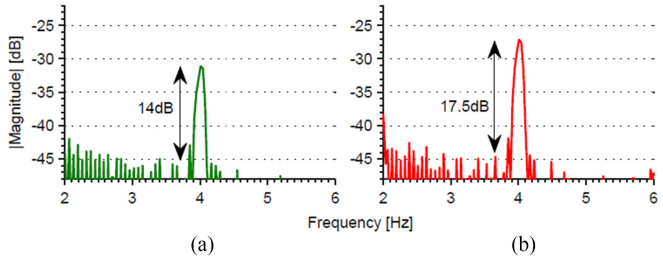

Fig. 6. Power spectral density estimation of the correlation coefficients: a) *Corr*(*G*) and b) *Corr*(*R*). The vibration source (with $\pm$5.6 μm amplitude, 2 Hz frequency and 20 s of duration) is located at point P_5.

Fig. 5 shows an illustrative example of the temporal behavior of both *Corr*(*G*) and *Corr*(*R*). The piezoelectric stack was located at point P_5 and it was excited with a driving signal with *Vpp* = 75 V and a mean value of 37.5 V, which represents a periodic perturbation of $\pm$5.6 μm.

Fig. 6 shows the corresponding power spectral density estimation of both *Corr*(*G*) and *Corr*(*R*) for the particular case illustrated in Fig. 5. It can be seen that the system is able to clearly identify the frequency response of a vibration source located at 5 m from the interrogation unit. It is also important to note that the piezoelectric stack is excited with a sinusoidal signal whose amplitude and mean values are *V* and *V/2*, respectively. Thus, the excitation signal generates a spatial displacement ($\pm\triangle$y) around the initial value which is defined by its mean value. The proposed sensor measures absolute spatial displacements with respect to the initial spatial position. For this reason, the correlation frequency (4 Hz) doubles the excitation frequency (2 Hz).

B. Improved Signal to Noise Ratio

The proposed remote sensing system employs a dual-wavelength technique which allows improving the signal–to–noise ratio of the measurements. *Corr*(*G*) and *Corr*(*R*) are independent signals taken at the same instant. So it is possible to reduce the random noise in the measurements by using a mixed correlation signal (i.e. by multiplying both signals, *Corr*(*G*) and

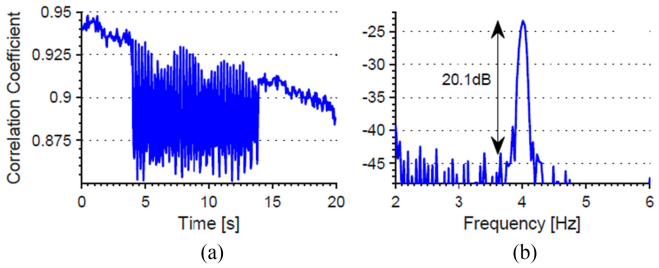

Fig. 7. a) Temporal behavior of the correlation signal (mixed signal) *GR*. b) Power spectral density estimation of *GR*. The vibration source (with ± 4 μm amplitude, 2 Hz frequency and 20 s duration) is located at the point P_5.

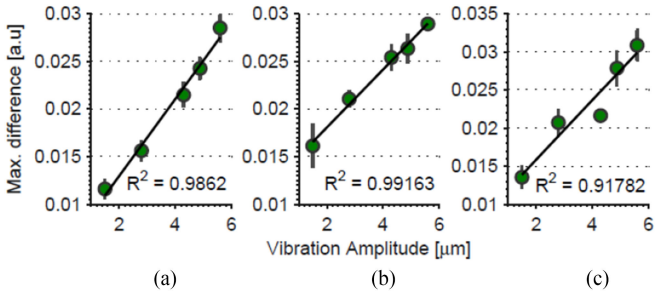

Fig. 8. Maximum variation of Corr(G) in the time domain when the vibration source is placed at points: a) P_1, b) P_5 and c) P_9.

Corr(*R*), respectively). This concept is illustrated in the results depicted in Fig. 7. While Fig. 7a shows the temporal variation of the signal *GR*, defined as $GR = Corr(G) \times Corr(R)$, Fig. 7b shows its power spectral density estimation. The product of both signals increases more than 2.6 dB the signal–to–noise ratio compared to the results shown in Fig. 6.

V. Results: Detection of Microvibrations

In this section the experimental results obtained from each wavelength as well as those obtained from the mixed signal are presented. At each sensing point (P_1, P_5 and P_9) four rounds of measurements were performed. Driving voltages (*V*pp) ranging from 15 V to 75 V during 10 s intervals were configured thus obtaining vibration amplitudes between ± 1.5 and ± 5.6 μm, respectively. The piezoelectric control signal is activated after starting the images recording; in this way, it is possible to measure the initial variation of the correlation coefficient which represents the initial displacement of the piezoelectric stack (see Fig. 5a and 5b). The results are shown in Figs. 8 and 9, respectively. The error bars shown within the figures represent the normalized mean square error (NMSE) of 4 different rounds of measurements.

A. Results for Single Wavelength Speckle Pattern

The graphs within Fig. 8 show the results of the maximum variation of the signal *Corr*(*G*) obtained when the vibration source is localized at points P_1, P_5 and P_9, respectively. It can be seen that *Corr*(*G*) can be approximated to a linear model with R^2 between 0.9178 and 0.9916. It is also observed that the maximum amplitude of the error bars is 2.2×10^{-3} a.u. and

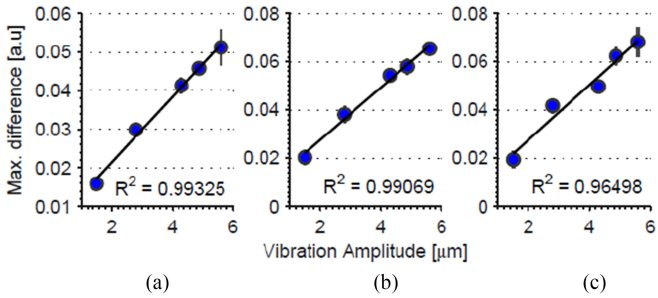

Fig. 9. Maximum variation of $GR = Corr(G) \times Corr(R)$ when the vibration source is placed at points: a) P_1, b) P_5 and c) P_9.

TABLE I
Summary of Results

Point	Signal	NMSE ($\times 10^{-3}$ a.u.) mean(1)	NMSE ($\times 10^{-3}$ a.u.) max(2)	Sensitivity ($\times 10^{-3}$ μm^{-1})	Resolution (μm)(3)	R^2
P_1	*Corr*(*G*)	1.10	1.30	6.690	0.164	0.986
	Corr(*R*)	1.66	4.31	7.577	0.219	0.892
	GR	1.66	4.31	**14.067**	**0.118**	**0.993**
P_5	*Corr*(*G*)	1.24	2.20	5.015	0.247	0.991
	Corr(*R*)	2.35	2.85	13.367	0.176	0.979
	GR	2.35	2.85	**17.960**	**0.131**	**0. 991**
P_9	*Corr*(*G*)	1.54	2.20	6.454	0.239	0.917
	Corr(*R*)	3.09	5.39	12.245	0.252	0.948
	GR	3.09	5.39	**18.871**	**0.164**	**0.965**

Notes: (1) Mean NMSE is calculated as the sum of the amplitudes of the error bars divided by the number of points, points = 5, at P_1, P_5 or P_9. (2) Max NMSR is calculated as the maximum amplitude of the error bars at P_1, P_5 or P_9. (3) Resolution is calculated as the minimum displacement that can be measured above the mean NMSE.

that a mean sensitivity of 6×10^{-3} a.u./μm is achieved. The maximum variation of the signal *Corr*(*R*) at the same conditions is also measured and results are reported on Table I.

B. Results for Mixed Signal

The graphs within Fig. 9 show the results of the maximum variation of the mixed correlation signal *GR*, where $GR = Corr(G) \times Corr(R)$, obtained when the vibration source is placed at points P_1, P_5 and P_9, respectively. *GR* can be approximated to a linear model. A better R^2 is obtained ranging between 0.9649 and 0.9932. The maximum amplitude of the error bars is kept below 5.39×10^{-3} a.u., and the mean sensitivity is increased to 16.97×10^{-3} a.u./μm (see Table I), which represents a relative improvement of 182% and 21.8% with respect to the sensitivity results obtained from the individual green and red speckle patterns, respectively.

VI. Discussion

A. Detection of Microvibrations with a Single Wavelength Approach

Table I summarizes the experimental results obtained employing a single wavelength approach as well as the proposed dual-wavelength speckle-based scheme.

Employing λ_2 in the single-wavelength approach a greater sensitivity can be obtained, however at the cost of reducing the

system resolution compared to perform the interrogation at a wavelength λ_1. This fact is in good agreement with the fact that measured modal noise penalty in an optical communications link is greater as the operating wavelength increased [13]. Additionally, the single wavelength approach at λ_1 shows a more linear regime compare to the λ_2 counterpart.

No matter the wavelength selected to operate the reflective-based proposed single wavelength approach, experimental resolutions well below 1 μm are achieved. Such a resolution value meets the requirements of most of the industrially available sensing applications. For instance, absolute position encoders offer 1 μm resolution if based on magnetic transducers or 0.5 μm if employing optical methods. FBGs resolutions [14] are also in that range unless more sophisticated and complex FBG post-processed systems with resolutions of $\sim$2.1 nm [15] are considered. Even state-of-the art computer mouse that uses speckle pattern analysis and specific signal processing reach lateral relative translation resolutions of 5 μm [16]

B. Dual-Wavelength Scheme With Enhanced Resolution and Linearity

By employing the dual-wavelength technique both linearity and system resolution can be enhanced compared to the single wavelength approach previously discussed while NMSE measurement error values are maintained. From the results shown in Table I with the novel proposed topology, a 30% resolution enhancement (evaluated at point P_9) can be achieved improving, at the same time, the linear behavior of the system up to $R^2 = 0.965$ compared to that of obtained for the single wavelength approach.

C. Applications

The particular characteristics of the speckle phenomenon have been reported in recent years for multiple sensing applications such as vibration sensing, displacement, distance, cracks in concrete structures or blood flow. Small size, ease of handling, biocompatibility, light weight, geometrical flexibility, chemical inertness, electric and thermal insulation and immunity to electromagnetic interference are inherent features of POF-based fiber-optic sensors. Biomedical applications, clinical biomechanics and the monitoring of physiological parameters are targeted as potentially suitable candidates to exploit the sensitivity and resolution performance obtained with the novel technique reported in this work. When continuous monitoring of critical parameters in day-to-day activities is required wireless portable interrogators can be cumbersome for both medical practitioners and patients [17] and a smart central monitoring for remote interrogation can be seen as a good choice. Additionally, the dual-wavelength approach aims to provide greater measurement robustness in the monitoring of the so-called medical vital signs, i.e. body temperature, pulse rate, respiration rate and blood pressure, where the muscular noise arises as the main error source [18].

Finally, the input optical power launched into the fiber sensing lead is -21.92 dBm (at 520 nm) and -19.05 dBm (at 650 nm), both well below eye-safety recommendations, according to ANSI-Z136.1 (2000) recommendations.

VII. Conclusion

A cost–effective method for sensing vibrations with a POF fiber lead is presented. The proposed technique detects periodical changes in the spatial distribution of energy on the speckle pattern in the output of the fiber. The topology includes off-the-shelf and low-cost devices such a laser pointer, a beam splitter cube that can be replaced by a POF coupler, a mirror and a webcam.

By employing a dual–wavelength approach it is possible to increase resolution and improve robustness to modal noise. The technique has been successfully demonstrated on different points of a 11 m-long SI–POF lead that operates in reflective configuration, thus providing a centralized interrogation scheme with improved sensitivity. It also allows a distributed sensing topology. The speckle pattern of both wavelengths is demultiplexed at the fiber end before being directly recorded by an off–the–shelf webcam and then post–processed by evaluating the ratio of the variances of the speckle patterns at the two different wavelengths. There is no need to use bare fiber, neither to reduce the number of modes to achieve a good resolution.

References

[1] H. Takahara, "Visibility of speckle patterns: Effect of the optical guide length in coherent light," *Appl. Opt.*, vol. 15, no. 3, Mar. 1976, Art. no. 609.

[2] R. Epworth, P. R. Couch, and J. M. T. Rowe, "The phenomenon of modal noise in analogue and digital optical fibre systems," in *Proc. 4th Eur. Conf. Opt. Commun.*, Genoa, Italy, 2013, pp. 492–501.

[3] A. Tapetado, D. S. Montero, D. Webb, and C. Vázquez, "A self-referenced optical intensity sensor network using POFBGs for biomedical applications," *Sensors*, vol. 14, no. 12, pp. 24029–24045, Dec. 2014.

[4] P. J. Pinzón, I. P. Garcilópez, and C. Vázquez, "Efficient multiplexer/demultiplexer for visible WDM transmission over SI-POF technology," *J. Light. Technol.*, vol. 33, no. 17, pp. 3711–3718, Sep. 2015.

[5] V. M. Sperandio, M. J. Pontes, A. F. Neto, and L. G. Webster, "A new optical pressure sensor interrogated by speckles pattern for oil industry," in *Proc. 24th Int. Conf. Opt. Fibre Sensors*, 2015, Art. no. 96347W.

[6] V. Trivedi *et al.*, "Optical temperature sensor using speckle field," *Sensors Actuators A Phys.*, vol. 216, pp. 312–317, Sep. 2014.

[7] P. Podbreznik, D. Donlagić, D. Lešnik, B. Cigale, and D. Zazula, "Cost-efficient speckle interferometry with plastic optical fiber for unobtrusive monitoring of human vital signs," *J. Biomed. Opt.*, vol. 18, no. 10, Oct. 2013, Art. no. 107001.

[8] J. Rohollahnejad, L. Xia, Y. Ran, and R. Cheng, "Deformation independent FBG strain sensor based on speckle pattern processing," in *Proc. 14th Int. Conf. Opt. Commun. Netw.*, 2015, pp. 1–3.

[9] C. Vazquez, J. Montalvo, D. S. Montero, and J. M. S. Pena, "Self-referencing fiber-optic intensity sensors using ring resonators and fiber bragg gratings," *IEEE Photon. Technol. Lett.*, vol. 18, no. 22, pp. 2374–2376, Nov. 2006.

[10] D. S. Montero, C. Vázquez, J. M. Baptista, J. L. Santos, and J. Montalvo, "Coarse WDM networking of self-referenced fiber-optic intensity sensors with reconfigurable characteristics," *Opt. Express*, vol. 18, no. 5, Mar. 2010, Art. no. 4396.

[11] L. Rodriguez-Cobo, M. Lomer, C. Galindez, and J. M. Lopez-Higuera, "Speckle characterization in multimode fibers for sensing applications," in *Proc. V Int. Conf. Speckle Metrology*, 2012, Art. no. 84131R.

[12] P. J. Pinzón, D. S. Montero, A. Tapetado, J. C. Torres, and C. Vázquez, "Dual-wavelength speckle-based SI-POF sensor for frequency detection and localization of remote vibrations," in *Proc. 6th Eur. Workshop Opt. Fibre Sensors*, 2016, Art. no. 99161Z.

[13] P. Pepeljugoski, D. Kuchta, and A. Risteski, "Modal noise BER calculations in 10-Gb/s multimode fiber LAN links," *IEEE Photon. Technol. Lett.*, vol. 17, no. 12, pp. 2586–2588, Dec. 2005.

[14] T. Guo, J. Albert, C. Chen, A. Ivanov, and A. Laronche, "Highly accurate micro-displacement measurement based on Gaussian-chirped tilted fiber Bragg grating," in *Proc. 19th Int. Conf. Opt. Fibre Sensors*, 2008, Art. no. 700417.
[15] M. Ferreira *et al.*, "Ultra-High sensitive strain sensor based on post-processed optical fiber bragg grating," *Fibers*, vol. 2, no. 2, pp. 142–149, Apr. 2014.
[16] Logitech, "G9X Logitech Laser Mouse." [Online]. Available: http://www.logitech.com
[17] J. Witt *et al.*, "Medical textiles with embedded fiber optic sensors for monitoring of respiratory movement," *IEEE Sens. J.*, vol. 12, no. 1, pp. 246–254, Jan. 2012.
[18] L. Burattini *et al.*, "Cleaning the electrocardiographic signal from muscular noise," in *Proc. 12th Int. Workshop Intell. Solutions Embedded Syst.*, 2015, pp. 57–61.

Plinio Jesús Pinzón received the B.S. degree in electronics and telecommunications engineering from the Technological University of Panama, in 2009, the M.Sc. degree (with first class Hons.) in advanced electronic systems from the Carlos III University of Madrid (Madrid, Spain) in 2011, and the Ph.D. degree in electrical, electronics and automation engineering from the Carlos III University of Madrid in 2015. He is currently working as Associate Professor at the Electronics Technology Department, Carlos III University of Madrid, as Member of the Displays and Photonic Application Group. His research interests include optical communications, and instrumentation including, plastic optical fibers, broadband access networks and monitoring techniques, filters, switches, fiber optic sensors, photonic devices based on liquid crystals, and WDM networks.

David Sánchez Montero was born in Seville, Spain, in 1978. He received the M.S. degree in telecommunications engineering from the University of Seville, Sevilla, Spain, in 2003 and the Ph.D. degree in electrical, electronics and automation engineering from Carlos III University of Madrid, Madrid, Spain, in 2011. From 2004 to 2012, he was a Teaching Assistant with the Electronics Technology Department, Carlos III University of Madrid as a Member of the Displays and Photonic Application Group, becoming Lecturer from 2012 to 2015. Since 2015, he has been an Associate Professor with the Electronics Technology Department, Carlos III University of Madrid. He is the author of one book, two book chapters, more than 60 papers in journals and conference proceedings, and two Spanish patents. He was a Visiting Researcher at ZHO-Universität Duisburg-Essen, Duisburg, Germany, INESC TEC, Porto, Portugal, DTU-Fotonik Metro-Access & Short Range Systems Division, Denmark, and the Research Laboratory of Electronics, Massachusetts Institute of Technology, Cambridge, MA, USA, working on different research topics. His research interests include fiber-optic sensors, polymer optical fibers, optical access networks and monitoring techniques, RoF systems, and WDM and FTTx networking. He has participated in different European projects and networks in the IST framework programme, such as EPhoton/One+, Building the Future Optical Network in Europe, and has participated in several national researching projects and consortiums.

Alberto Tapetado received the M.Sc. degree in industrial electronics engineering from the University of Castilla-La Mancha, Ciudad Real, Spain, in 2009, and the Ph.D. degree in electrical engineering, electronics and automation from Carlos III University of Madrid, Leganés, Spain, in 2015. He was a visiting student at Aston Institute of Photonics Technologies in Aston University, Birmingham, United Kingdom, in 2012, and at the Research Laboratory of Electronics in the Massachusetts Institute of Technology, Cambridge, USA, in 2013; working on polymer optical fiber Bragg gratings and silicon photonics, respectively. He is currently working as Postdoctoral Researcher at Electronics Technology Department of Carlos III University of Madrid, as a member of the Displays and Photonic Application Group. His research interests focus on polymer and silica fiber optics sensors, sensor networks, integrated optics, and broadband access networks.

Carmen Vázquez (M'99–SM'05) received the M.Sc. degree in physics (electronics) from the Complutense University of Madrid, Madrid, Spain, in 1991, and the Ph.D. degree in photonics at the Telecommunications Engineering School, Universidad Politécnica of Madrid, Madrid, Spain, in 1995. She enjoyed a fellowship at TELECOM, Denmark, in 1991, working on erbium-doped fiber amplifiers. From 1992 to October 1995, she worked at the Optoelectronics Division, Telefónica Investigación y Desarrollo, Madrid, Spain. She was involved in III-V integrated optics devices characterization, design, and fabrication. In October 1995, she joined University Carlos III of Madrid, Spain, where she is currently a Full Professor at the Electronics Technology Department and the Head of the Displays and Photonic Applications Group. She was Visiting Scientist at the Research Laboratory of Electronics in the Massachusetts Institute of Technology from August 2012 to July 2013, working on silicon photonics. She was also the Head of Department for three years and Vice-Chancellor for four years. Her research interests include integrated optics, optical communications, and instrumentation including, polymer optical fibers, broadband access networks and monitoring techniques, RoF systems, filters, switches, fiber optic sensors, and WDM networks. She is a Fellow of the SPIE and she has published more than 250 papers in journals and conference proceedings and is the holder of 7 patents. She has participated in different European projects and networks in the ESPRIT, RACE, and IST framework programmes, such as PLANET, OMAN, HEMIND, SAMPA, EPhoton/One+, Building the Future Optical Network in Europe, etc., and has leaded several national researching projects and consortium such as SINFOTON-CM.